Fibers and Polymers 2018, Vol.19, No.4, 877-886
DOI 10.1007/s12221-018-7875-y

ISSN 1229-9197 (print version)
ISSN 1875-0052 (electronic version)

Azo Dye Removal Using Free and Immobilized Fungal Biomasses: Isotherms, Kinetics and Thermodynamic Studies

Gulay Bayramoglu[1,2]* and Meltem Yilmaz[3]

[1]*Biochemical Processing and Biomaterial Research Laboratory, Gazi University, Ankara 06500, Turkey*
[2]*Department of Chemistry, Faculty of Sciences, Gazi University, Ankara 06500, Turkey*
[3]*Department of Biology, Faculty of Arts and Sciences, Gazi University, 06900 Polatlı, Ankara, Turkey*
(Received October 14, 2017; Revised January 18, 2018; Accepted March 2, 2018)

Abstract: In this study, *Lentinus concinnus* biomass was immobilized in polyvinyl alcohol/polyethyleneoxide hydrogels (PVA/PEO; referred as composite biomass) and used for removal of Reactive Yellow 86 dye (RY-86) from aqueous solution using free fungal biomass as a control system. The free fungal and composite fungal biomasses were characterized using ATR-FTIR, SEM and analytical methods. FTIR studies of the adsorbent preparations show that carboxylate, hydroxyl and amine groups should be involved in adsorption of the RY-86 dye. The adsorption of RY-86 dye on these adsorbents increased as the initial concentration of RY-86 dye in the medium increased up to 200 mg/*l*. The maximum RY-86 dye adsorption for the free fungal and composite fungal biomasses, was obtained as 190.2 and 87.6, respectively, using 200 mg/*l* initial dye concentration, at 25 °C, and at pH 5.0 with 2.0 h contact. The equilibrium data were well described with the Freundlich and Temkin isotherm models. The adsorption of RY-86 dye was fitted best by the pseudo second-order kinetic model. Thermodynamic parameters (ΔG^{o}, ΔH^{o}, and ΔS^{o}) showed that RY-86 dye adsorption on both adsorbents were spontaneous process.

Keywords: Composite biomass, Reactive Yellow 86, Adsorption, Isotherms, Kinetics, Thermodynamics

Introduction

Environmental pollution caused by the toxic organic and inorganic compounds (such as synthetic dyes, pesticides, drugs, and heavy metals) is a matter of great concern [1]. The synthetic dyes are mostly utilized in the foods, cosmetics, papers, and textiles industries [2]. Among them, the azo dyes are characterized by the presence of azo bonds, aromatic rings, and sulfate and amino groups. Wastewaters containing dyes are highly colored and these effluents impair the living things in the aquatic systems. Azo dyes are generally recalcitrant due to their xenobiotic character and exhibit significant resistance to microbial degradation [3,4]. For removal of dyes from wastewaters several methods have been proposed for removal of the organic pollutants from wastewaters such as adsorption [5-8], microbial and enzymatic degradation [9-12], and chemical processes [13]. For adsorption of micro-pollutants, many different composite adsorbents have been synthesized using natural polymers such as chitin, alginate, cellulose, and their derivatives and synthetic polymers such as poly(vinyl alcohol), poly (ethyleneimine), and poly(acrylic acid) [7,8]. For example, a composite adsorbent can be easily prepared by combination of microbial biomass with one of these polymers via immobilization techniques and can improve the adsorbent performance and adsorption capacity. Different types of microbial biomasses such as fungi, bacteria, yeast, and algae were immobilized with a goal of finding more effective composite adsorbent [14,15]. Among them, white rot fungus biomasses have been shown to be economic materials, as they can be easily cultivated using cheap and abundant carbon sources such as cellulose. In additions, they have high organic pollutant adsorption capacities due to the presence of several functional groups on their cell surfaces such as amino, hydroxyl, carboxyl, and sulfate, which can act as binding sites for the various organic/inorganic pollutants [14,16]. In the last years, composite adsorbents have received great interest due to their potential applications in industrial wastewater treatment due to the cumulative effects of each component and also exhibited high performance for removal of micro-pollutants [17]. Polyvinyl alcohol (PVA) is a hydrophilic polymer and has been used in food industry as food packaging material, in chemical engineering for preparation of resins and coating agents, and in medical area for production of surgical threads. The PVA based hydrogels can be stabilized using various polymers such as polyethylene oxide and can be utilized for entrapment of cells or enzyme under mild experimental conditions [18,19].

Recently, many different types of composite adsorbents have been prepared and used to clean up the aquatic environment. For the preparation of composite adsorbents, natural and synthetic materials have been combined to enhance the removal capacity of the resulting absorbent. For example, composites of polyaniline, starch, polypyrrole, chitosan aniline, and chitosan pyrrole using peanut waste were prepared and used for the adsorption of Crystal Violet dye from aqueous media [20]. *Pyracantha coccinea* biomass was modified with an anionic surfactant and used for Methyl Violet dye removal studies [21]. Polyaniline/starch composite was synthesized and used for removal of Actacid Orange-

*Corresponding author: g_bayramoglu@hotmail.com

RL in batch mode [22]. Altıntıg *et al.* prepared a composite adsorbent from magnetic particles and activated carbon and used for removal of Methylene Blue from aqueous medium [23]. Rice bran composites were prepared with polyaniline, starch, polypyrrole, chitosan aniline, and chitosan pyrrole and employed for the adsorption of Malachite green dye [24]. A novel composite adsorbent was prepared from poly(glycidylmetharylate-ethyleneglycol dimethacrylate) and magnetic particles and employed for the adsorption of Reactive Green 5 and Reactive Brown 10 dyes [25]. A novel mango stone biocomposite adsorbent was prepared and utilized for the adsorption of Crystal Violet dye from aqueous solution [26]. A composite adsorbent was prepared from carboxymethyl cellulose and fungal biomass and employed for removal of Disperse Red 60 [27]. Native, HCl pre-treated clay and $MnFe_2O_4$/clay composite were synthesized and successfully utilized as an adsorbent for removal of Methyl Green from aqueous solution [28].

In this study, the free and composite biomass of *L. concinnus* were prepared and used for removal of RY-86 dye from aqueous solution by using bare PVA/PEO hydrogel as a control system. The effect of initial dye concentration, adsorption time, adsorbent dosage, and pH was evaluated. The Langmuir, Freundlich, Dubinine Radushkevich (D-R), and Temkin isotherm models were used for fitting of the experimental adsorption data. Three kinetic models (i.e., pseudo first-order, pseudo second order, and Elovich) were used to evaluate the mechanism of adsorption. Thermodynamic parameters such as ΔG^o, ΔH^o, and ΔS^o were also calculated.

Experimental

Materials

Reactive Yellow 86 (RY-86) was obtained from Sigma-Aldrich Chem. Co., St. Louis, MO, USA, and the chemical structure and properties of the RY-86 dye are presented in Table 1. Polyvinyl alcohol (PVA) and polyethylene oxide (PEO; CAS Number: 25322-68-3) were also obtained from Sigma-Aldrich Chem. Co. All other chemicals were of analytical grade and purchased from Merck AG (Darmstadt, Germany).

Immobilization of *L. concinnus* Biomass in PVA-PEO Hydrogel

The white rot fungus *Lentinus concinnus* "MAFF 430305" was obtained from the National Institute of Agrobiological Sciences, Tsukuba, Ibaraki, Japan. The fungal biomass was harvested from the growth medium by filtration. It was washed with sterile saline solution and stored at 4 °C until use.

PVA (5.6 g) and PEO (3.4 g) were mixed together with deionized water (37 m*l*) and heated at 95 °C until PVA dissolved completely. The mixture was cooled down to 30 °C, and fungal biomass about 4.0 g was added and mixed. The PVA/PEO-fungal biomass mixture was extruded through a needle (radius 1.0 mm) onto a Teflon® plate surface and dried in an incubator up to 30 % of its initial mass. Then, PVA-PEO preparations were soaked in sodium sulfate solution (0.1 mol/*l*; stabilizing solution) for re-swelling about 4.0 h [14]. The composite PVA-PEO-fungal biomass was washed with acetate buffer (pH 5.0, 50 mmol/*l*) and stored at 4 °C in the same buffer until use. Immobilization protocols are presented in Figure 1.

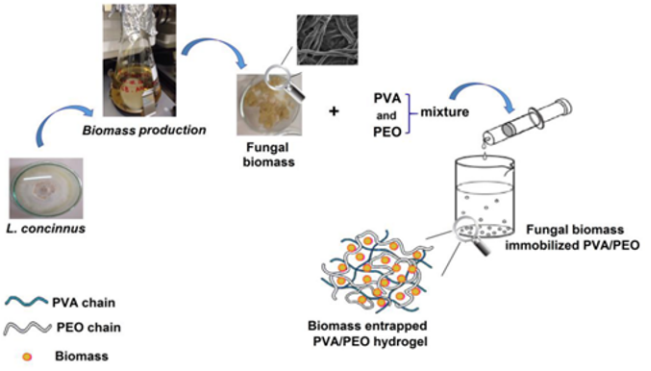

Figure 1. Immobilization protocol of fungal biomass in PVA/PEO hydrogel.

Adsorption Studies of RY-86 Dye

The effects of pH and adsorbent dosage on the dye removal efficiency were studied by changing medium pH from 1.0 to 9.0 and by varying adsorbent dose between (0.1 and 2.0 g/*l*), respectively. The effect of contact time was studied in the range 5 to 120 min. The effect of temperature and ionic strength was studied at four different temperatures (i.e. 15, 25, 35, and 45 °C) and at different NaCl concentrations between 0.1 and 1.0 mol/*l* at pH 5.0. The effect of initial concentration of dye on the adsorption capacity was studied by varying the concentration of dye between 10 and 300 mg/*l*. All these experiments were conducted in duplicates with 10 mg adsorbent sample. Adsorption experiments were carried out 10 mg adsorbent in 10 m*l* of dye solution (200 mg dye/*l*) at 25 °C for 2.0 h. The dye concentration in the solution was analyzed using a double beam UV/vis spectrophotometer (PG Instrument Ltd., Model T80+; PRC). Calibration curve was obtained by plotting absorbance (A428) of the dye versus concentration.

Elution and Regeneration of the Adsorbents

Adsorption-desorption cycles were repeated ten times by using the same adsorbent preparation. Desorption of dye was performed by 50 mmol/*l* $NaCO_3$ solution. The dye laden free or composite fungal biomass preparations were transferred in desorption medium and stirred at 150 rpm for 2.0 h at 25 °C. After each cycle of adsorption-desorption, the adsorbent

preparations were washed with 0.1 mol/*l* NaCl solution and transferred into fresh dye solution.

Characterization of Adsorbents

ATR-FTIR spectra of the free fungal biomass, bare PVA-PEO and composite fungal biomass were obtained by using an attenuated total reflectance-Fourier-transform infrared (ATR-FTIR) spectrometer (Nicolet IS 5, Thermo Electron Scientific Instruments, WI, USA).

The surface morphology of the sample was examined using a scanning electron microscope (SEM). The dried sample was mounted on a stamp and coated with a thin layer of gold for 3.0 min. The samples were then placed in a SEM holder and their scanning electron micrographs were obtained using a SEM microscope (ZEIZZ, Evo 50). The surface of the sample was scanned at the desired magnification to observe the morphology of the samples.

Results and Discussion

Properties of the Adsorbents

In order to predict the functional groups responsible for RY-86 dye adsorption, ATR-FTIR spectroscopy was used. The ATR-FTIR spectra of free fungal biomass, bare PVA-PEO, and composite fungal biomass are presented in Figure 2. The FT-IR spectra of free biomass of *L. concinnus* have intense peaks at 3244 cm^{-1} which was assigned to the stretching vibration of hydroxyl groups and also stretching vibration of -NH groups (Figure 2(a)). The peaks at 2919 cm^{-1} can be attributed to C-H stretching vibrations. The strong peaks at around 1635 cm^{-1} are caused by the bending of N-H of the chitin moiety of the fungal biomass. The peaks at 1900 cm^{-1} can be assigned as aromatic ring substitution overtones, and the peaks at 1358 and 1015 cm^{-1} represent $-CH_3$ and C-OH stretching vibrations, respectively (Figure 2(a)). The FT-IR spectrum of bare PVA-PEO hydrogel is presented in Figure 2(c). The bands observed between 3400 and 3200 cm^{-1} are linked to the stretching vibration of O-H groups. The vibration band 2914 cm^{-1} can be associated with the stretching vibration of C-H from alkyl groups. The peaks at 1690, 1371, and 1231 cm^{-1} can be associated with the stretching C=O, C-O, and -OH group of PVA and PEO, respectively. The similar peaks were observed for the composite fungal biomass (Figure 2(c)).

The SEM micrographs of free fungal biomass, bare PVA-PEO hydrogel, and composite fungal biomass are presented in Figure 3(a), (b), and (c), respectively. As can be seen from these figures, the SEM image of fungal biomass shows multi-cellular hyphae forming mycelium. This property can be considered as a factor providing an increase in the surface area. Hence, it is expected to lead a high adsorption capacity for the dye (Figure 3(a)). The SEM image of bare hydrogel was completely different from the fungal biomass immobilized counterpart (Figure 3(b)). A uniform fungal biomass distribution was observed indicating that immobilization of fungal biomass was not localized (Figure 3(c)).

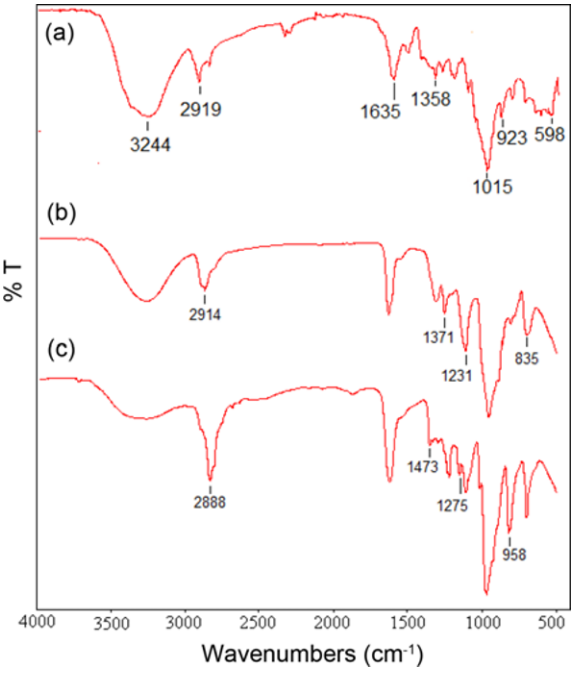

Figure 2. ATR-FTIR spectra; (a) free fungal biomass, (b) bare PVA-PEO hydrogel, and (c) composite fungal biomass in hydrogel.

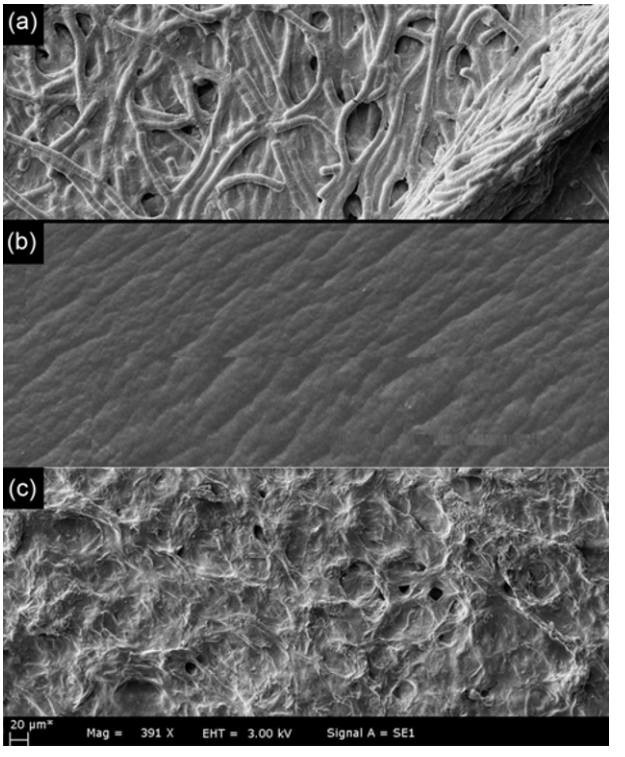

Figure 3. SEM images; (a) free fungal biomass, (b) bare PVA-PEO hydrogel, and (c) composite fungal biomass.

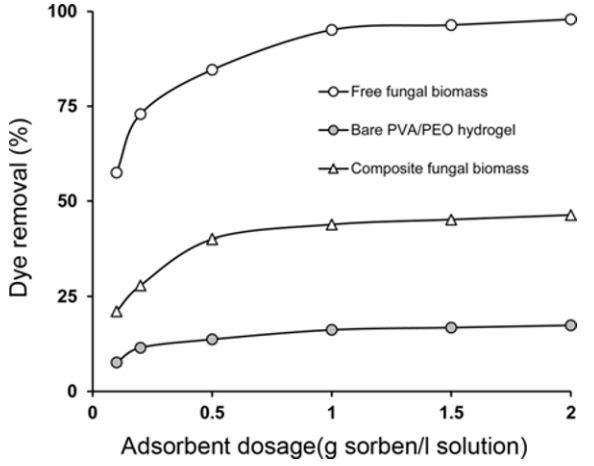

Figure 4. Effect of adsorbent amount on the adsorption of the dye on bare PVA-PEO hydrogel, free fungal biomass, and composite fungal biomass.

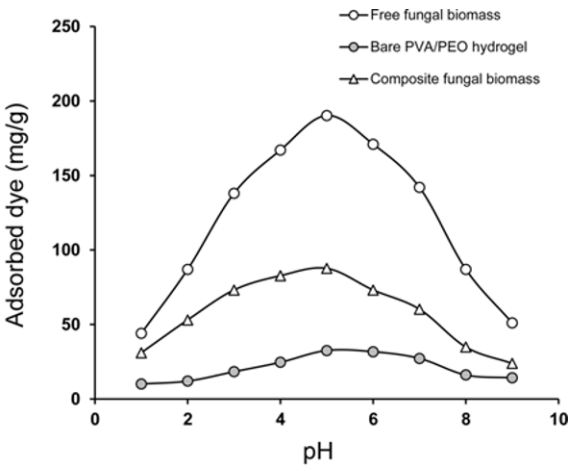

Figure 5. Effect of pH on the dye adsorption of the RY-86 dye on bare PVA-PEO hydrogel, free fungal biomass, and composite fungal biomass.

Effect of Adsorbent Dosage

The removal capacity of Reactive Yellow 86 dye was studied by varying the adsorbents dosage between 0.1 and 2.0 g/*l* at a constant dye concentration of 200 mg/*l* and at pH 5.0 (Figure 4). As can be seen from this figure, the amount of dye adsorbed varied with initial sorbent dosage, and increased with the increasing the adsorbent dosage. The removal percentage of the free, composite fungal biomass, and bare PVA-PEO hydrogel were found to be 97.6, 46.3 and 17.4 %, respectively. At sorbent dosages >1.0 g/*l*, the increase in percent removal of dye with increase in the adsorbent dose was less. Therefore, 1.0 g/*l* adsorbent dose was used in the remaining studies. It should be noted that the increase in the percent dye removal with increase in the adsorbent dose can be caused by the greater availability of the adsorptive sites.

Effect of pH on Dye Adsorption

The fungal cell walls contain chitin/chitosan, proteins, lipids, and melanin and these macromolecules contain many adsorptive sites such as amino, carboxyl, thiol, phosphate, and hydrophobic groups. These functional groups are capable of bonding to dye molecules [2,20]. It should be noted that the ionization states of these functional groups in the adsorption medium depend on the medium pH [8,29]. The maximum adsorption of dye on the bare PVA-PEO hydrogel, free and composite fungal biomasses was observed at pH 5.0, and found to be 32.5, 190.2 and 87.6 mg/g, respectively. As can be seen from Figure 5, the adsorption of the dye on the adsorbent preparations increased up to pH 5.0. The RY-86 is an azo dye and has two sulfates, a primary and a secondary amino group, several hydrophobic entities, and hydrogen donor groups for bonding to the adsorbent preparations (Table 1). The pK_a value of the sulfate and the

Table 1. The general characteristics of Reactive Yellow 86

IUPAC Name of dye	4-[(2Z)-2-(5-carbamoyl-1-ethyl-4-methyl-2,6-dioxopyridin-3-ylidene)hydrazinyl]-6-[(4,6-dichloro-1,3,5-triazin-2-yl)amino]benzene-1,3-disulfonate
Synonym	Procion Yellow MX8G
Color index number	C.I.192755
Chemical formula	$C_{18}H_{14}Cl_2N_8Na_2O_9S_2$
	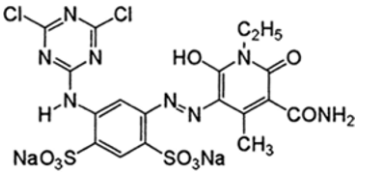
Molecular weight (g/mol)	667.357
Chemical/Dye Class	Single azo
λ_{max} (nm)	428 nm

$-NH_2$ groups of the dye molecule is 1.87 and 9.5, respectively. These functional groups can be readily dissociated under the studied pH values, and thus, the dye molecule has zwitterion form in the studied pH range. The adsorption capacities of the used adsorbents were found to be increased up to pH 5.0 whereas the amount of adsorbed dye was observed to be decreased at pH>5.0. In earlier studies, similar observation for the adsorption of dyes on the various adsorbents were reported [20,22]. For example, composite of carboxymethyl cellulose-fungal biomass was used for removal of Direct Red 60. However, at lower pH values the carboxyl groups of the composite adsorbent were protonated, reducing dye binding sites [34].

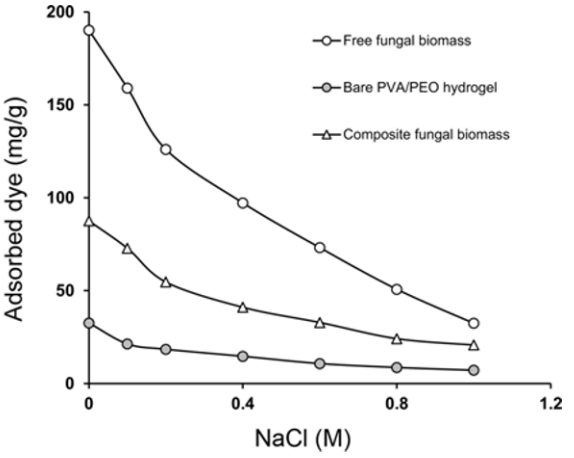

Figure 6. Effect of ionic strength on the dye adsorption on bare PVA-PEO hydrogel, free fungal biomass, and composite fungal biomass.

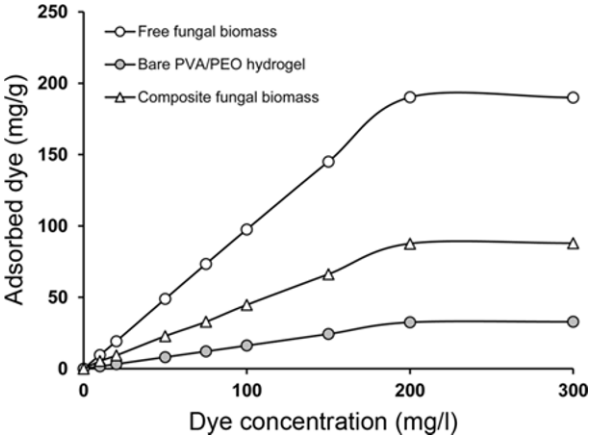

Figure 7. Effect of initial dye concentration on the adsorption capacity of on bare PVA-PEO hydrogel, free fungal biomass, and composite fungal biomass.

Effect of Ionic Strength on Dye Adsorption

Textile effluents contain a notable amount of salt which may influence the removal of dyes from solution. The effect of ionic strength on the dye removal was realized at pH 5.0 with bare PVA-PEO hydrogel, the free and composite fungal biomasses. When the electrostatic forces between sorbent functional groups and adsorbate molecules are opposite, an increase in salt concentration will cause a reduction in the adsorption capacity of adsorbent [30]. The ionic strength of the adsorption medium was changed between 0.00 and 1.0 M by varying salt concentration. As can be seen in Figure 6, for all the tested adsorbents, the amount of dye adsorbed decreased with increasing ionic strength. This can be due to the decrease electrostatic attraction between dye molecules and the adsorptive groups of adsorbents. An increase in the amount of Na^+ and Cl^- ions in the adsorption medium can screen the charged sites of the adsorbent and the electric double layers of the adsorbents surface are compressed, leading to a reduction in the electrostatic interactions, and thus a decrease in the amount of the dye adsorbed was observed [16]. This observation shows that ion-exchange could be responsible for the RY-86 adsorption process for the tested adsorbents.

Effect of Initial Dye Concentration and Isotherm Models Studies

The adsorption capacities of the free, composite fungal biomass, and bare PVA-PEO hydrogel are presented in Figure 7 as a function of the initial concentration of the dye within the solutions. As can be seen from the figure, the adsorption capacity of the tested adsorbents was enhanced with increasing the initial concentration of dye, and reached saturation values of 200 mg/*l*. The amount of dye adsorbed on bare hydrogel was found to be 32.5 mg/g, whereas the amounts of adsorbed dye on the free fungal and immobilized fungal biomass were found to be 190.2 and 87.6 mg/g, respectively. The order of the dye adsorption capacity of the adsorbents was found to be: free fungal biomass > composite fungal biomass > bare PVA-PEO hydrogel. In the previous studies, similar observation for dye for dyes adsorption onto various composite adsorbents have been reported [20-26]. It should be noted that the increase in initial dye concentration can cause an increase in the capacity of the adsorbent, and this can be due to the high driving force for mass transfer at a high initial dye concentration [31,32]. However, beyond this concentration, the binding sites can be saturated and target pollutant adsorption slowed down [33,34,37].

The experimental data was analyzed with four different isotherm models, namely, Langmuir, Freundlich, Dubinin-Radushkevich (D-R), and Temkin. The used isotherm models equations are:

The linear form of Langmuir isotherm model equation:

$$C_e / q_e = C_e / q_{max} + 1/(q_{max} \cdot b) \quad (1)$$

where q_{max} is the maximum adsorption capacity (mg/g), C_e is the equilibrium RY-86 dye concentration in solution (mg/*l*), and b is the Langmiur constant.

The linear Freundlich isotherm model equation:

$$\ln q_e = (1/n) \ln C_e + \ln K_F \quad (2)$$

where K_F and n are the Freundlich adsorption isotherm constants.

The Dubinin-Radushkevich (D-R) equation is described for adsorption nonporous, macro-porous, and mesoporous adsorbents. The linear D-R isotherm model equation:

$$\ln q_e = \ln q_D - B_D[RT \ln (1 + 1/C_e)]^2 \quad (3)$$

where B_D is related to the free energy of adsorption and q_D is the D-R isotherm constant related to the degree of adsorption by the adsorbent.

Table 2. Adsorption isotherm models constants for adsorption of RY-86 on the bare PVA-PEO hydrogel and free and composite fungal biomasses from aqueous solution

		Model parameters			
	Biosorbent	q_{max} (mg/g)	$b\times10^3$ (*l*/mg)	R^2	*R_L
Langmuir	Bare PVA-PEO hydrogel	197.1	266.9	0.785	0.622
	Free fungal biomass	163.9	6.61	0.998	0.362
	Composite fungal biomass	135.9	5.89	0.918	0.335
		K_F	n	R^2	
Freundlich	Bare PVA-PEO hydrogel	0.24	1.08	0.992	
	Free fungal biomass	37.3	1.97	0.989	
	Composite fungal biomass	1.52	1.22	0.994	
		q_D (mg/g)	$B_D\times10^5$ (J/mol)	R^2	E (kJ/mol)
D-R	Bare PVA-PEO hydrogel	17.3	3.40	0.934	4.77
	Free fungal biomass	137.0	0.03	0.916	6.99
	Composite fungal biomass	45.6	1.12	0.911	6.27
		Q_T	$K_T\times10^1$ (*l*/mg)	R^2	b_T (kJ/mol)
Temkin	Bare PVA-PEO hydrogel	9.98	0.86	0.944	0.09
	Free fungal biomass	37.1	15.0	0.911	0.07
	Composite fungal biomass	24.7	1.52	0.942	0.10

*Initial concentrations (C_o) of RY-86: 300 mg/*l*.

The Temkin isotherm is based on the assumption that heat of adsorption would decrease linearly with increase of coverage of adsorbent due to adsorbate/adsorbent interactions [2,29].

The linearized Temkin isotherm equation:

$$q_e = Q_T \ln K_T + Q_T \ln C_e \quad (4)$$

where $Q_T = RT/b_T$, b_T is the Temkin constant related to heat of adsorption (kJ/mol), K_T is the Temkin isotherm constant (*l*/g), R is the gas constant (8.314 J/mol·K), and T is the Kelvin temperature (K).

The calculated isotherm models parameters are presented in Table 2. The Langmuir isotherm is the most widely used isotherm model. The calculated Langmuir constants and correlation coefficients are presented in Table 2. Relatively large deviations were observed between the experimental isotherm data and the calculated values, especially in all the concentration, and the tested temperature ranges, and correlation coefficients were also found to be out of the statistical analysis range. One of the possible reason for the dissimilarity of experimental data with Langmuir isotherm constants is that Langmuir isotherm is based on the adsorption phenomena of surface layering on the homogeneous surface. This is not the case for the adsorption of RY-86 dye on the free and immobilized fungal biomasses. In addition, the essential characteristic of the Langmuir isotherms was expressed in terms of a dimensionless constant separation factor or equilibrium parameter, R_L, which is defined in equation (5)

$$R_L = 1/(1 + b\ C_o) \quad (5)$$

The R_L values between 0 and 1 indicate favorable absorption. Also, R_L values equal to 0 indicate irreversible absorption, $R_L = 1$ is linear, and $R_L > 1$ is unfavorable. In this study, R_L values for RY-86 dye adsorption on the free fungal biomass, composite fungal biomass, and bare PVA-PEO hydrogel surfaces ranged from 0.335 to 0.622 (Table 2). As observed from this table, the adsorption of RY-86 dye on the adsorbent preparations was seem to be feasible.

The higher correlation coefficients of Freundlich model than those of the Langmuir and D-R equations reveal that the adsorption data can be well described by the Freundlich model (Table 2). From the linear plots of Freundlich model constants (i.e., K_F and n) for bare PVA-PEO hydrogel, the free and composite fungal biomasses, positive cooperativity in binding and heterogeneous nature of adsorption (Values of $n > 1$ for the RY-86 dye at 25 °C) were indicated. R^2 was higher than those of the other isotherm models (Table 2). K_F and n are indicative of the extent of the adsorption and the degree of non-linearity between solution concentration and adsorption, respectively.

D-R isotherm was also applied to plots of equilibrium adsorption data for all adsorbents. Values of D-R constants, q_D and B_D, for the adsorption of RY-86 dye on the free fungal, composite fungal biomasses, and bare PVA-PEO hydrogel surfaces calculated from the intercept and slope of the plots are presented in Table 2. The correlation coefficients were equal and less than 0.934 (Table 2). The B_D value gives

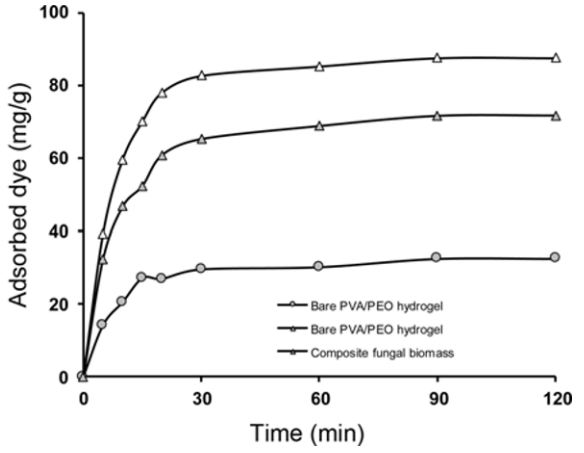

Figure 8. Effect of contact time on the adsorption of the RY-86 dye on bare PVA-PEO hydrogel, free fungal biomass, and composite fungal biomass.

information about the mean free energy E (kJ/mol) of adsorption per molecule of the adsorbate and can be calculated using the relationship ($E = 1/(2\,B_D)^{1/2}$). It is reported that the E value is small than 8.0 kJ·mol^{-1}, the adsorption process can be considered as the physical adsorption [16]. It was clear that the adsorption energy value was lowest for adsorption of RY-86 dye on the tested adsorbent preparations. From Table 2, it can be noticed that the calculated values of mean free energy (E) are inadequate within the range of 4.77-6.27 kJ/mol. In this case, the D-R model does not fit well the experimental data.

Temkin isotherm model was also applied to the experimental data to determine the heat of adsorption (b_T, kJ/mol) of the tested adsorbent preparations (Table 2). The constant b_T reflects bonding energy which in turn dictates the type of interaction. In our study low values of b_T (between 0.07 and 0.10 kJ/mol) for bare PVA-PEO hydrogel, the free, and composite fungal biomasses indicate that interactions between the RY-86 dye and the used adsorbents are neither purely through ion-exchange nor purely through physical-adsorption.

Adsorption Time and Kinetic Models

The equilibrium adsorption time of the RY-86 dye on bare PVA-PEO hydrogel, the free biomass, and composite fungal biomass from aqueous solution was investigated in a batch system. Figure 8 shows the adsorption time of the RY-86 dye on the adsorbent preparation from solutions containing 200 mg/*l* dye. The initial removal of the RY-86 dye was fast, which could be attributed to the unsaturated surface of the adsorbent preparations. Equilibrium was reached after 60 min. After this time period, the concentration of adsorbed RY-86 dye did not considerably change further with contact time.

The kinetic data was analyzed with three different kinetic models (i.e., pseudo-first-order, pseudo-second-order, and the Elovich equations). These models equations are presented in equations (6), (7), and (8), respectively.

$$\log (q_e - q_t) = \log q_e - (k_1 \cdot t) / 2.303 \quad (6)$$

$$(t/q_t) = (1/k_2\, q_e^{\,2}) + (1/q_e)\, t \quad (7)$$

$$q_t = (1/\beta)\ln (\alpha\,\beta) + (1/\beta)\ln t \quad (8)$$

where q_e (mg/g) and is the experimental amount of dye adsorbed at equilibrium, q_t (mg/g) is the amount of dye adsorbed at time t, k_1 (min^{-1}) and k_2 (g/mg/min) are the equilibrium rate constants of the pseudo first- and second-

Table 3. Kinetic parameters for adsorption of RY-86 on the bare PVA-PEO hydrogel and free fungal and composite fungal biomasses from aqueous solution

		Model parameters				
	Biosorbent	$q_{e,exp}$ (mg/g)	$q_{e,cal}$ (mg/g)	$k_1\times10^1$ (min^{-1})	R^2	
First-order	Bare PVA-PEO hydrogel	32.5	22.9	6.81	0.929	
	Free fungal biomass	190.2	81.1	7.03	0.987	
	Composite fungal biomass	87.6	67.6	8.12	0.962	
		$q_{e,exp}$ (mg/g)	$q_{e,cal}$ (mg/g)	$k_2\times10^1$ (g/mg min)	$h\times10^{-2}$ (g/mg min)	R^2
Second-order	Bare PVA-PEO hydrogel	32.5	34.2	5.14	0.06	0.987
	Free fungal biomass	190.2	196.2	1.43	0.55	0.994
	Composite fungal biomass	87.6	91.7	2.31	0.19	0.979
			α (mg/g min)	$\beta\times10^2$ (g/mg)	R^2	
Elovich	Bare PVA-PEO hydrogel		0.35	18.9	0.925	
	Free fungal biomass		0.45	3.60	0.916	
	Composite fungal biomass		0.96	7.15	0.953	

order kinetic models, respectively. The constant k_2 is used to calculate the initial adsorption rate h (mg/g/min) at $t \rightarrow 0$ by using $h = k_2 q_e$. The application of the pseudo-second order kinetics by plotting t/q_t versus t yields the second order rate constant k_2. For Elovich equations, α is the initial adsorption rate (mg/g/min) and the parameter β is related to the extent of surface coverage and activation energy for adsorption (g/mg). The constants of the pseudo-first-order, pseudo-second-order, and Elovich equations are presented in Table 3.

The same experimental data are also plotted with the pseudo second order kinetic equation and the results are shown in Table 3. If pseudo-second order kinetics are applicable, the plot of t/q_t against t of equation (7) should give a linear relationship, from which $q_{e,cal}$, k_2, and h can be determined from the slope and intercept of the plot. The correlation coefficients are 0.987, 0.994, and 0.979 for bare PVA-PEO hydrogel, free biomass, and composite fungal biomass, respectively. Comparison of the R^2 values for used three different equations suggested that dye adsorption by the bare PVA-PEO hydrogel, free biomass, and composite fungal biomass followed the pseudo-second-order kinetic model. As can be seen from this table, the correlation coefficients (R^2) obtained from the pseudo-second-order model were found to be higher than 0.979, making them larger than those of the pseudo-first-order and Elovich models. The results obtained from the pseudo-second-order model described best the experimental data of the applied kinetic models. In addition, the calculated adsorption capacities (q_e) using the pseudo-second-order model agreed with the corresponding experimental adsorption capacities of the used adsorbent preparations. The plot was found to be linear for all the tested adsorbents with much lower correlation coefficient (>0.916) indicating that the Elovich equation represented the poorer fit of experimental data than that of the pseudo-second-order model equations.

Thermodynamic Parameters

The temperature of the adsorption medium could be important for energy dependent mechanisms in pollutant removal by adsorbent. In this work, the adsorption of RY-86 dye by bare PVA-PEO hydrogel, free biomass, and composite fungal biomass was found to be temperature dependent between 15 and 45 °C, and the maximum binding values of the used adsorbents were increased with increasing temperature (Table 4).

The reason for the increase in the dye adsorption on the adsorbent preparations (bare hydrogel, free, and immobilized fungal biomass) at high temperatures could be attributed to increase in the interaction between dye molecules and functional groups on the adsorbent surfaces. These results also indicated that the adsorption of dye is an endothermic process [2,9]. Also, the solubility and chemical potential of adsorbate are related to temperature; higher temperature facilitates the adsorption of pollutants on adsorbents because the mobility of the substance interacts more effectively with the functional groups (to enhance the rate of protonation and deproptonation) on the prepared adsorbent [9]. The values of the equilibrium adsorption constant ($K_a = b$; the association coefficient) which can be calculated by using Langmuir equation (1)) in M^{-1} unit were calculated according to the following equation:

K_a = Dye concentration in the sorbent at equilibrium (mg/g) / Dye concentration in solution at equilibrium (mg/l) × Molecular weight of dye (mol/g) (9)

Table 4 shows the variation in K_a values for RY-86 dye adsorption on the bare PVA-PEO hydrogel, free fungal biomass, and composite fungal biomass as changing tem-

Table 4. The distribution coefficient and adsorption constants and the thermodynamic parameters for adsorption of RY-86 on the bare PVA-PEO hydrogel and free fungal and composite fungal biomasses from aqueous solution at different temperatures

Biosorbent	T (K)	q_{exp} (mg/g)	$K_a \times 10^{-3}$ (M^{-1})	ΔG^o (kJ/mol)	ΔH^o (kJ/mol)	ΔS^o (kJ/mol K)
Bare PVA-PEO hydrogel	288	29.70	0.12	-11.4	7.46	0.065
	298	32.50	0.13	-12.1		
	308	34.80	0.14	-12.7		
	318	38.10	0.16	-13.4		
Free fungal biomass	288	177.40	5.24	-20.5	71.8	0.320
	298	190.20	13.0	-23.4		
	308	195.30	27.8	-26.2		
	318	198.60	94.7	-30.3		
Composite fungal biomass	288	77.80	0.42	-14.5	10.8	0.088
	298	87.60	0.53	-15.5		
	308	92.20	0.57	-16.3		
	318	99.40	0.66	-17.2		

peratures. Their values were found to be increase by increasing temperature of the adsorption medium.

The following equations have been used to determine the thermodynamic parameters such as enthalpy (ΔH^o), Gibbs free energy (ΔG^o) and entropy (ΔS^o).

$$\Delta G^o = -RT \ln K_a \quad (10)$$

$$\ln K_a = -\Delta G^o/RT = -\Delta H^o/RT + \Delta S^o/R \quad (11)$$

where R is the gas constant (8.314 J/mol/K) and T represents the absolute temperature (K). The values of ΔH^o and ΔS^o were determined from the slope and intercept of the van't Hoff plot of $\ln K_a$ versus $1/T$.

The values of the thermodynamic parameters are presented in Table 4. The negative values of ΔG^o suggested that the adsorption process was spontaneous, and the decreasing of ΔG^o with the increasing of temperature indicated that the adsorption was more favorable at high temperatures. The positive values of ΔH^o confirmed the endothermic process for the adsorption of RY-86 dye, consistent with the increase of adsorption capacity as temperature increased. The positive value of ΔS^o suggested that the increasing randomness between the solid/solution interface during the adsorption process.

Desorption Studies

In order to determine the reusability of the adsorbent preparations, consecutive adsorption-desorption cycles were repeated ten times by using the same adsorbent. Desorption of RY-86 dye was performed by using 50 mmol/*l* Na_2CO_3 solution. Each dye laden adsorbent preparation was placed in the desorption medium and stirred at 150 rpm for 2.0 h at 25 °C. After each adsorption-desorption cycle, the adsorbent preparation was washed with 0.1 mol/*l* NaCl solution, and transferred into fresh RY-86 dye solution for operation next cycle. When 50 mmol Na_2CO_3 solution was used for desorption of RY-86 dye from the adsorbents (i.e., the free fungal biomass, composite fungal biomass, and bare PVA-PEO hydrogel), 71.6, 79.3, and 92.9 % desorption was obtained, respectively. It should be noted that the electrostatic interaction between functional groups of adsorbents and RY-86 dye decreased at alkaline pH resulting in desorption of adsorbed dye.

In order to show the reusability of the used adsorbents, the adsorption-desorption cycle was repeated ten times with the same sorbent preparation [14]. Adsorption capacity of the free fungal biomass, composite fungal biomasses, and bare PVA-PEO was decreased about 28.4, 20.7, and 7.1 % in the first cycle. On the other hand, there were gradual decrease in RY-89 dye adsorption with an increase in the number of cycles, and these were more pronounced for the free and immobilized fungal biomass preparations [16,34-37]. Thus, the adsorption capacities of the tested sorbent preparations were gradually reduced in the subsequent cycles. After ten cycles, the RY-86 dye removal performance by the free, composite fungal biomasses, and bare PVA-PEO was reduced by 58, 63, and 19 % compared to their initial adsorption capacities, respectively.

Conclusion

Immobilized microorganism technology creates opportunities in a wide range of areas including environmental pollution control, biotechnological area, and fermentation industries. Immobilized microorganisms have many advantages compared to their free counterpart, such as reusability, easy separation, and stability to toxic chemicals. The adsorption of the RY-86 dye on the free fungal and composite fungal biomasses depended on the experimental conditions particularly medium pH and the concentration of RY-86 dye in the solutions. The Freundlich and Temkin isotherm models described well the experimental adsorption data and followed the pseudo-second-order kinetic model for the tested adsorbents. The reusability test indicated that the presented adsorbents can be used as low cost and effective adsorbents for dye removal from aqueous solutions. Also, the composite fungal biomass can be used as an effective adsorbent for the removal of organic pollutant from wastewaters.

Acknowledgements

This work was supported by the Research Programs of Gazi University (PAB-Grand No:18/2015-01) Turkey, Ankara. The authors wish to thanks to National Institute of Agrobiological Sciences (NIAS) for supplying the white-rot fungus (*Lentinus concinnus*).

References

1. N. K. Singh, A. S. Raghubanshi, A. K. Upadhyay, and U. N. Rai, *Ecotoxicol. Environ. Saf.*, **130**, 224 (2016).
2. G. Bayramoglu and M. Y. Arica, *J. Hazard. Mater.*, **143**, 135 (2007).
3. M. T. Chaudhry, M. Zohaib, N. Rauf, S. S. Purves, and S. Tahir, *Appl. Microbiol. Biotechnol.*, **98**, 3133 (2014).
4. F. Guzel, H. Saygılı, G. Akkaya-Saygılı, F. Koyuncu, and C. Yılmaz, *J. Clean. Prod.*, **144**, 260 (2017).
5. T. A. Arica, E. Ayas, and M. Y. Arica, *Microporous Mesoporous Mater.*, **243**, 164 (2017).
6. G. Bayramoglu, B. Altintas, and M. Y. Arica, *Chem. Eng. J.*, **152**, 339 (2009).
7. N. M. Mahmoodi, O. Masrouri, and F. Najafi, *Fiber. Polym.*, **15**, 1656 (2014).
8. G. Bayramoglu and M. Y. Arica, *Bioresour. Technol.*, **100**, 186 (2009).
9. S. Sadaf, H. N. Bhatti, S. Nausheen, and S. Noreen, *Arch. Environ. Contam. Toxicol.*, **66**, 557 (2014).
10. U. Kalsoom, H. N. Bhatti, and M. Asgher, *Appl. Biochem.*

Biotechnol., **176**, 1529 (2015).
11. M. Y. Arica, B. Salih, O. Celikbicak, and G. Bayramoglu, *Chem. Eng. Res. Des.*, **128**, 107 (2017).
12. P. Zhang, Q. Wang, J. Zhang, G. Li, and Q. Wei, *Fiber. Polym*., **15**, 30 (2014).
13. G. Bayramoglu, B. Karagoz, and M. Y. Arica, *J. Ind. Eng. Chem.*, **60**, 407 (2018).
14. G. Bayramoglu and M. Y. Arica, *Water Air Soil Pollut*., **221**, 391 (2011).
15. S. Mirnezhad, S. Safapour, and M. Sadeghi-Kiakhani, *Fiber. Polym*., **18**, 1134 (2017).
16. G. Bayramoglu and M. Y. Arica, *J. Radioanal. Nucl. Chem*., **307**, 373 (2016).
17. P. Dvorak, S. Bidmanova, J. Damborsky, and Z. Prokop, *Environ. Sci. Technol*., **48**, 6859 (2014).
18. E. J. Espinosa-Ortiz, E. R. Rene, K. Pakshirajan, E. D. van Hullebusch, and P. N. L. Lens, *Chem. Eng. J*., **283**, 553 (2016).
19. D. S. Franklin and S. Guhanathan, *Ecotoxicol. Environ. Saf*., **121**, 80 (2015).
20. N. Tahira, H. N. Bhattia, M. Iqbal, and S. Noreena, *Int. J. Biol. Macromol*., **94**, 210 (2017).
21. S. T. Akar, F. Sayin, S. Turkyilmaz, and T. Akar, *Environ. Sci. Pollut. Res*., **21**, 13055 (2014).
22. S. Noreen, H. N. Bhatti, M. Zuber, M. Zahid, and M. Asgher, *Pol. J. Environ. Stud.* **26**, 2125 (2017).
23. E. Altıntıg, H. Altundag, M. Tuzen, and A. Sarı, *Chem. Eng. Res. Des.,* **122**, 151 (2017).
24. H. N. Bhatti, A. Jabeen, M. Iqbal, S. Noreen, and Z. Naseem, *J. Mol. Liq.*, **237**, 322 (2017).
25. G. Bayramoglu, A Akbulut, G Liman, and M. Y. Arica, *Chem. Eng. Res. Des.*, **124**, 85 (2017).
26. S. Shoukat, H. N. Bhatti, M. Iqbal, and S. Noreen, *Microporous Mesoporous Mater*., **239**, 180 (2017).
27. G. Bayramoglu, V. C. Ozalp, and M. Y. Arıca, *Water Sci. Technol.*, **75**, 366 (2017).
28. A. Ehsan, H. N. Bhatti, M. Iqbal, and S. Noreen, *Water Sci. Technol.*, **75**, 753 (2017).
29. H. Asnaoui, A. Laaziri, and M. Khalis, *Water Sci. Technol*., **72**, 1505 (2015).
30. X. Yang, K. Chen, Y. Zhang, H. Liu, W. Chen, and J. Yao, *Fiber. Polym.*, **18**, 1652 (2017).
31. A. Rashid, H. N. Bhatti, M. Iqbal, and S. Noreen, *Ecol. Eng.*, **91**, 459 (2016).
32. M. A. Tahir, H. N. Bhatti, and M. Iqbal, *J. Environ. Chem. Eng.*, **4**, 2431 (2016).
33. M. Mushtaq, H. N. Bhatti, M. Iqbal, and S. Noreen, *J. Environ. Manage*., **176**, 21 (2016).
34. J.-Z. Guo, B. Li, L. Liu, and K. Lv, *Chemosphere*, **111**, 225 (2014).
35. G. Bayramoglu and M. Y. Arica, *Fiber. Polym*., **13**, 1225 (2012).
36. G. Bayramoglu, A. Akbulut, I. Acıkgoz-Erkaya, and M. Y. Arica, *J. Appl. Phycol*., https://doi.org/10.1007/s10811-017-1238-8 (2017).
37. G. Bayramoglu, A. Akbulut, and M. Y. Arica, *Water Sci. Technol.*, **74**, 914 (2016).